IJHSR
ijhighschoolresearch.org
RESEARCH ARTICLE

Application of NASA's General Mission Analysis Tool (GMAT) in Replicating and Optimizing Historical Interplanetary Trajectories

Adesh Krishnan

St. Joseph Institution International, 490 Thomson Rd, Singapore 298191, adeshkrishnan0@gmail.com
Mentor: Steve Bullock

ABSTRACT: This study investigates the limitations of numerical optimization tools in replicating historical interplanetary mission trajectories. Using NASA's General Mission Analysis Tool (GMAT), two gravity-assist missions, Voyager 2 and Pioneer 11, were reconstructed based on publicly available ephemeris data and mission parameters. Historical estimates of the total delta-v (Δv) required for all Trajectory Correction Maneuvers (TCMs) were derived from published propellant mass and engine performance data. These values were compared to the total Δv generated by GMAT-simulated equivalents of each mission. In both cases, GMAT produced trajectories that required significantly higher total TCM Δv than the historical missions despite attempts at further optimization. These results demonstrate a clear divergence between numerical solver outputs and the solutions implemented during the original missions. The discussion examines potential causes for this discrepancy, including the limitations of GMAT's numerical solvers in planning and optimizing interplanetary space missions.

KEYWORDS: Engineering Mechanics, Aerospace and Aeronautical Engineering, Physics, Orbital Mechanics, Spacecraft Mission Planning.

Introduction

Gravity assists have played a critical role in enabling highly efficient interplanetary trajectories, allowing spacecraft to reach distant targets that would otherwise be inaccessible with available propulsion technology. By carefully maneuvering a spacecraft to pass close to a planet, mission planners can exploit the planet's gravity to alter the spacecraft's velocity and trajectory without expending large amounts of fuel. This technique has been pivotal in advancing deep space exploration, enabling missions to maximize scientific returns within the mass and power constraints of available launch vehicles.[1,2]

Designing such missions is an incredibly complex task. The trajectory must be timed with precision to ensure that each planetary encounter produces the desired change in velocity and trajectory. Even small deviations in timing or position can compound over large distances, leading to missed encounters or large corrective maneuvers downstream.

Two early examples of successful gravity-assist missions are NASA's Pioneer 11 and Voyager 2. Pioneer 11 launched on April 5th, 1973, and relied on a Jupiter flyby for a gravitational boost towards Saturn and completed its flyby of Saturn in September 1979 (a mission duration of over six years). It became the first spacecraft to closely study Saturn, revealing new findings including Saturn's outermost ring (the F ring), an additional moon, and the composition of Saturn's atmosphere.[3]

Voyager 2 launched on August 20th, 1977, and executed a historic "Grand Tour" of the outer planets, including flybys of all four gas giants over approximately twelve years (Neptune flyby in August 1989). It remains the only spacecraft to visit both Uranus and Neptune, capturing the first up-close images and data from these planets. Voyager 2 discovered Neptune's Great Dark Spot, fastest planetary winds, six new moons, and four rings, marking groundbreaking advances in our understanding of the outer solar system.[4]

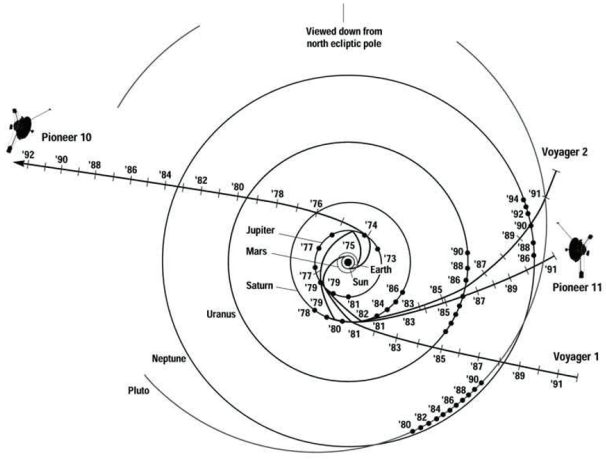

Figure 1: Trajectories of the Pioneer and Voyager spacecraft in the solar system, viewed from above the north ecliptic pole (*NASA – Public Domain*).[5]

The mission design tools available in the 1970s were far more limited than those in use today. In the 1960s–70s, trajectory planning relied more on analytical methods and approximations, as the computer technology of the time made high-fidelity numerical simulations infeasible. Mission analysts manually applied celestial mechanics equations, which led to forced approximations. By the 1990s, advances in computing power and numerical methods led to the development of more sophisticated mission-planning software, enabling broad

DOI: 10.36838/IJHSR87.230

numerical searches that could evaluate vastly more trajectory options. This shift made possible missions such as Genesis and Dawn, which required capabilities beyond what 1970s technology could support. Today, even basic computers can integrate full equations of motion and simulate complete gravitational models, making numerical optimization the standard for trajectory design. Nevertheless, important limits remain: gravity-assist tours are typically sought via time-consuming, broad numerical searches over many possible flyby combinations, and the discrete nature of these searches means it is still easy to step past promising trajectories. As a result, analysts may be uncertain whether a mission concept is fully optimized or whether the software missed a better solution.[6]

NASA's General Mission Analysis Tool (GMAT) is a prominent example of this kind of software. It is a modern, open-source mission design software capable of spacecraft trajectory propagation and optimization.[7] GMAT represents a class of software that became available in the late 20th and early 21st century, along with other powerful trajectory design software such as JPL's Mission Analysis, Operations, and Navigation Toolkit Environment (MONTE) and Astrogator.[7,8]

This study addresses the application of NASA's General Mission Analysis Tool (GMAT) in replicating and optimizing historical interplanetary trajectories. Understanding the capabilities and limitations of GMAT in this context is essential for accurately assessing the performance of modern trajectory optimization software, setting realistic expectations for its use in both reproducing past missions and supporting the planning of future ones. By comparing GMAT-generated trajectories with the actual results of historically successful missions, this research aims to evaluate how contemporary numerical optimization tools perform when tasked with designs originally produced under the technological and operational constraints of earlier eras.

Hypothesis:

In this study, mission efficiency will be evaluated using the total Δv from all TCMs required to complete each spacecraft's trajectory. This Δv will serve as a proxy for fuel consumption, providing a quantifiable metric for comparing simulated results against historical missions. For Voyager 2 and Pioneer 11, historical TCM Δv estimates will be derived from published propellant mass and specific impulse (Isp) data, as exact recorded values are unavailable.

GMAT's numerical solvers will be used to replicate each mission's original planetary encounter sequence, which in this case is from Earth to Jupiter, Saturn, Uranus, and finally Neptune (EJSUN) for Voyager 2 and the Earth to Jupiter, then Saturn sequence for Pioneer 11. GMAT will then calculate the TCM Δv for each optimized trajectory, and the summed maneuver Δv values will be compared directly with historical estimates. This will provide insight into GMAT's capabilities and limitations in replicating and optimizing historical interplanetary missions.

It is hypothesized that GMAT's numerical solvers will not only replicate but also potentially optimize the trajectories of these missions by reducing total TCM Δv relative to historical estimates, thereby improving fuel efficiency.

Background:

Numerical vs. Analytical Methods:

Analytical methods in orbital mechanics aim to solve the equations of motion using exact mathematical expressions. These rely on simplifying the problem, such as reducing it to a two-body interaction, so that the equations can be solved directly. However, realistic missions rarely allow for purely analytical solutions because the required assumptions, such as neglecting relativistic corrections or solar radiation pressure, will reduce how accurately the model represents the real mission environment.[10]

Numerical methods, on the other hand, calculate spacecraft motion step-by-step, updating the position and velocity over small intervals of time based on the forces acting at each step. This process, known as numerical integration, produces an approximate solution that can be made more accurate by reducing the step size. Before digital computers, these calculations were done manually using finite-difference formulas, which required function values from several previous steps to start a new calculation. These "start-up procedures" made it difficult to change the step size during integration.[11]

Runge–Kutta methods, which do not require values from earlier steps, became popular because they were easier to apply at the start of an integration and allowed greater flexibility, such as changing the step size mid-calculation. While too laborious for hand computation, they became practical and widely used once digital computer software such as GMAT could perform the repetitive calculations quickly.[11]

GMAT:

GMAT is an open-source trajectory optimization and design system developed by NASA, available for anyone worldwide to download free of charge along with comprehensive documentation. It supports a wide range of mission types and is one of NASA's most expansive and successful software projects.[12]

At the core of GMAT's simulation capability are its propagators, which numerically integrate a spacecraft's equations of motion from given initial conditions. These propagators implement various numerical integration methods, including Runge–Kutta, as discussed earlier. Users have control over the integration step size, with smaller steps generally improving accuracy at the cost of increased computation time, and larger steps reducing computation time but potentially accumulating greater numerical error.

In addition to propagators, GMAT uses solvers that iteratively adjust mission parameters such as burn magnitudes or event timings until specific constraints, like target planetary flyby conditions, are met. Complementing these are optimizers, which systematically refine variables to minimize or maximize a chosen objective function, such as total Δv. Both solvers and optimizers approach trajectory design in a similar way, where the control inputs must be discovered through repeated simulation until the software converges on a suitable solution.

GMAT operates on a batch execution model, where users write and execute scripts to generate outputs, with modifications requiring direct edits to the script, followed by re-running the program. To accommodate users with varying levels of coding expertise, GMAT offers both a script-based environment and a Graphical User Interface (GUI). The GUI provides interactive features, including 3D visualizations and animations, enabling users to explore mission parameters intuitively. The scripting language follows a MATLAB®-like syntax, easing adoption for those familiar with that environment.[13]

In practice, GMAT users construct missions by defining resources, such as spacecraft, propagators, and optimizers, then configuring them to the mission's requirements. These elements are combined into a mission sequence, which models the spacecraft's motion, manoeuvres, and key events over time.

The VNB Axis and the B-Plane in Planetary Flybys:

The Velocity, Normal, and Binormal (VNB) reference frame is a spacecraft-centered local orbital reference frame that rotates with the spacecraft along its trajectory. In this reference frame, the x-axis is fixed to the velocity vector, which is tangent to the spacecraft's trajectory, pointing in the direction of motion. The y-axis will be perpendicular to the velocity vector and the orbital plane of the spacecraft, thus aligned with the angular momentum vector. The z-axis will be perpendicular to both vectors and lies within the orbital frame.[14] The geometry of this reference frame is depicted in Figure 2 below:

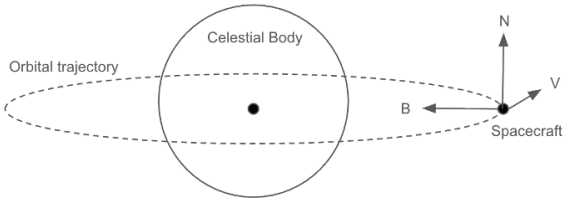

Figure 2: Velocity, Normal, Binormal (VNB) Reference Frame in Orbital Mechanics.

The B-plane is a conceptual plane used in planetary flyby analysis, defined as the plane perpendicular to the spacecraft's incoming asymptote vector. The asymptote represents the straight-line path that the spacecraft would follow if the planet's gravity were absent; it describes the direction of the spacecraft's velocity infinitely far from the planet, often denoted as v_∞. In other words, while the actual spacecraft follows a curved hyperbolic trajectory around the planet, the asymptote is the idealized line that the trajectory approaches at great distances.[15]

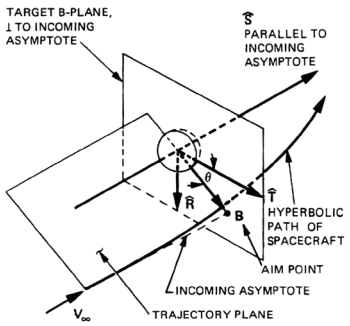

Figure 3: Geometric definition of the B-plane (*NASA – Public Domain*).[16]

As shown in Figure 3, the point where this incoming asymptote intersects the B-plane is called the aim point. This point serves as a convenient way to describe and control the geometry of the flyby, since small variations in the aim point correspond to significant changes in the spacecraft's outgoing trajectory after the planetary encounter. The B-plane is often expressed in terms of two unit vectors, $\hat{T}$ and $\hat{R}$, which span the plane. The spacecraft's B-vector, which represents the displacement of the asymptote relative to the planet, can be projected onto these two directions. These projections are called BdotT and BdotR, and they are mathematically defined as the dot products of the B-vector with the respective unit vectors (BdotT = $B\cdot\hat{T}$, BdotR = $B\cdot\hat{R}$). Conceptually, this means that BdotT measures displacement along the tangential direction, controlling how much the spacecraft's orbital energy changes, whereas BdotR measures displacement along the radial direction, driving changes in the inclination of the flyby trajectory.[15,17]

In practical mission design, it is crucial to understand that when engineers "target" a specific BdotT and BdotR in software such as GMAT, they are not directly moving the spacecraft itself. Instead, they are specifying where on the B-plane the aim point should fall. The optimizer then works backwards to determine the maneuver parameters (for example, Δv magnitude and timing) that adjust the spacecraft's actual trajectory so that its incoming asymptote intersects the B-plane at the desired coordinates. In other words, by shifting the aim point, one is indirectly controlling key aspects of the flyby: the turning angle, the closest approach distance, and the outbound trajectory. This makes the B-plane framework powerful, since it translates the complexity of a 3D gravity assist into a 2D targeting problem.

Gravity Assists and the Oberth Effect:

From a physics perspective, the gravity assist works because of the conservation of momentum and energy in a two-body interaction. When the spacecraft approaches a planet, it is captured temporarily into the planet's gravitational field and follows a hyperbolic trajectory relative to that planet. In the planet's frame of reference, the spacecraft comes in with some velocity, swings around the planet, and leaves with the same speed but in a different direction. However, when viewed in the Sun's inertial frame, the planet itself is not stationary but orbiting the Sun at high velocity. Because of this, the spacecraft effectively "borrows" a small portion of the planet's orbital momentum around the Sun.[18] This process can be better illustrated by considering velocity addition in different reference frames.[19] Let $\vec{v_p}$ be the planet's orbital velocity around the Sun, and $\vec{v}_{\infty in}$ and $\vec{v}_{\infty out}$ the incoming and outgoing hyperbolic excess velocities of the spacecraft relative to the planet.

In the planet's frame, the spacecraft's speed is conserved:

$$|\vec{v}_{\infty\, in}| = |\vec{v}_{\infty\, out}| \quad (1)$$

When transformed back into the heliocentric (Sun-centered) frame, the spacecraft's velocity is:

$$\vec{v}_{SC\, in} = \vec{v}_p + \vec{v}_{\infty\, in} \text{ and } \vec{v}_{SC\, out} = \vec{v}_p + \vec{v}_{\infty\, out} \quad (2)$$

DOI: 10.36838/IJHSR87.230

Thus, the change in the kinetic energy of the spacecraft can be written as:

$$\Delta E = \frac{1}{2}m(|\vec{v}_{SC\ out}|^2 - |\vec{v}_{SC\ in}|^2) \quad (3)$$

Then, by using the expression $|\vec{a}+\vec{b}|^2 = |\vec{a}|^2+|\vec{b}|^2+2\vec{a}\cdot\vec{b}$ and rearranging,

$$\begin{aligned} |\vec{v}_{SC\ out}|^2 - |\vec{v}_{SC\ in}|^2 &= |\vec{v}_p + \vec{v}_{\infty\ out}|^2 - |\vec{v}_p + \vec{v}_{\infty\ in}|^2 \\ &= |\vec{v}_p|^2 + |\vec{v}_{\infty\ out}|^2 + 2\vec{v}_p \cdot \vec{v}_{\infty\ out} - |\vec{v}_p|^2 - |\vec{v}_{\infty\ in}|^2 - 2\vec{v}_p \cdot \vec{v}_{\infty\ in} \\ &= 2\vec{v}_p \cdot (\vec{v}_{\infty\ out} - \vec{v}_{\infty\ in}) \end{aligned} \quad (4)$$

The last dot-product expression shown here is generally not zero because the outgoing and incoming spacecraft velocity vectors have the same magnitude but different directions. Therefore, this shows that a directional change relative to the planet is necessary in order to manipulate the heliocentric speed of the spacecraft.[20]

If the spacecraft is deflected forward, in the same direction as the planet's orbital motion, the dot product is positive: the spacecraft gains kinetic energy, effectively "stealing" a tiny fraction of the planet's orbital momentum. If deflected backward, opposite to the planet's motion, the dot product is negative: the spacecraft loses energy and slows down relative to the Sun. Therefore, gravity slingshots require a trajectory that brings the spacecraft past the planet on the side aligned with its orbital motion to increase speed.

Another important concept for maximizing the efficiency of fuel usage for interplanetary missions is the Oberth Effect, which explains why propulsive maneuvers are most efficient when performed at periapsis (the point of closest approach in an orbit), where the spacecraft is traveling at its fastest as compared to any other point along its trajectory due to the acceleration from gravity as it falls inwards closer to the planet. At higher orbital speeds, a given amount of propellant energy is converted into a disproportionately larger gain in kinetic energy. This is because kinetic energy scales with the square of velocity, so adding the same Δv at periapsis is the most efficient, as it results in the greatest increase in orbital energy.[21]

Tsiolkovsky Rocket Equation:

The performance of rockets is governed by the Tsiolkovsky rocket equation.[22] In this investigation, the equation will be used to estimate the total Δv of all TCM burns implemented during a mission, using the known fuel mass and the specific impulse of the propulsion system. The equation is written as:

$$\Delta v = I_{sp} \times g_0 \times ln(\frac{m_0}{m_f}) \quad (5)$$

Where:

Δv = the total change in velocity the rocket can achieve

I_{sp} = specific impulse of the propulsion system (seconds), a measure of the engine–fuel system's efficiency

g_0 = standard Earth gravity (9.81 m/s^2)

m_0 = initial mass of the spacecraft (with propellant)

m_f = final mass (after propellant has been expended)

Methodology

The first stage involved calculating the theoretical Δv requirements for each mission using the Tsiolkovsky Rocket Equation. This approach was adopted because no published data exist for the total Δv associated with all midcourse correction manoeuvres. For each spacecraft, published values for the mass at launch, current mass, and the engine's specific impulse were obtained from NASA mission archives and peer-reviewed literature. Substituting these values into the rocket equation yielded approximate Δv requirements based on the expended propellant for each vehicle, providing a value for comparison with the simulated mission.

For Voyager 2, NASA's Voyager Backgrounder lists a hydrazine tank mass of 104 kg and a mission module mass of 825 kg (which includes the hydrazine).[23] Currently, NASA claims that the approximate mass of Voyager 2 is 735 kg, meaning roughly 80 kg of hydrazine has been used.[24] Additionally, Voyager 2 used Aerojet MR-103 hydrazine monopropellant thrusters with I_{sp} of ~202-224 s. Hence, the implied Δv capacity is:[25,26]

$$\Delta v = \frac{202+224}{2} \times 9.81 \times ln(\frac{825}{735}) \quad (6)$$

$$\Delta v = 241.4\ m/s$$

For Pioneer 11, a peer-reviewed analysis reported launch mass of ~258 kg with ~27-30 kg of propellant aboard. In a 2002 JPL study, it was stated that the spacecraft performed major trajectory correction maneuvers on the way to Jupiter and Saturn, which resulted in about 20 kg of propellant being used.[27] Although the exact model of the propulsion system is publicly unavailable, it is known that it also utilized hydrazine monopropellant fuel, which means it had an I_{sp} which could range anywhere from ~180–285 s:[26,28]

$$\Delta v = \frac{180+285}{2} \times 9.81 \times ln(\frac{258}{238}) \quad (7)$$

$$\Delta v = 184\ m/s$$

In the second stage, this study incorporated published ephemeris data for Voyager 2 and Pioneer 11 in the form of SPK (Spacecraft and Planet Kernel) files obtained from NASA's SPICE archive. These kernels contain the precise spacecraft trajectory information referenced to the solar system barycenter, allowing accurate reconstruction of each mission within GMAT.[29] From these reconstructed runs, the key mission parameters required for replication were extracted, particularly the spacecraft's initial starting conditions and the B-plane coordinates (BdotT and BdotR) at each planetary flyby. These values served as the primary constraints for ensuring the simulated missions followed the same geometry as the actual flights. Table 1 below presents the acquired BdotT and BdotR values at each planetary flyby for the replicated missions.

Table 1: Primary simulation data showing the BdotT and BdotR values generated from GMAT for each flyby in the replicated Voyager 2 and Pioneer 11 missions.

Voyager 2		
Mission Stage	**BdotT [km]**	**BdotR [km]**
Jupiter Periapsis	1 913 212.28	167 664.27
Saturn Periapsis	324 486.32	-173 812.23
Uranus Periapsis	92 533.50	-87 205.31
Neptune Periapsis	-27 884.25	-41 724.75
Pioneer 11		
Mission Stage	**BdotT [km]**	**BdotR [km]**
Jupiter Periapsis	-371 218.72	473 675.46
Saturn Periapsis	335 609.29	19 526.29

The third stage was to construct the replicated mission in GMAT. To achieve this, the following targeting sequence was implemented:

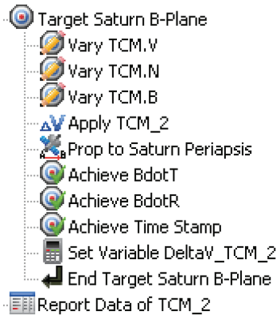

Figure 4: Targeting sequence for TCM 2, performed at Jupiter periapsis to satisfy Saturn B-plane targets.

Figure 4 is an excerpt from the mission sequence, which only shows the specific targeting loop structure used to correct Voyager 2's trajectory. However, all other TCMs across both missions followed the same loop structure, with only the timing and target conditions differing. To provide clarity, Table 2 summarizes the location and purpose of each TCM used in the replication of Voyager 2. Since Pioneer 11 followed a shorter trajectory that terminated at Saturn, only TCM 1 (the initial post-injection clean-up to set up Jupiter) and TCM 2 (the Jupiter-periapsis maneuver to target Saturn's B-plane and timing) were required. The latter TCMs listed at Saturn and Uranus periapsis apply only to Voyager 2, which continued to Uranus and Neptune.

Table 2: TCM Locations and Purposes.

TCM	Location of Execution	Purpose
TCM 1	Beginning of the simulated mission (post-injection cleanup)	Sets up the Jupiter encounter
TCM 2	Jupiter periapsis	Targets Saturn B-plane (BdotT/BdotR) and epoch
TCM 3	Saturn periapsis	Targets Uranus B-plane and epoch
TCM 4	Uranus periapsis	Targets Neptune B-plane and epoch

Each trajectory correction begins by propagating the spacecraft from its current state to the location of the manoeuvre. A target sequence is then defined, with the solver iteratively adjusting the burn components until the encounter geometry is met. The varied parameters are the three Δv components in the VNB frame. These are initially set to zero, and the solver determines their actual values. The burn is then applied, and the trajectory is propagated forward to the next planetary periapsis. At periapsis, the constraints are specified: the B-plane coordinates (BdotT and BdotR) and the timestamp of the flyby. The solver continues adjusting the three Δv components until these are satisfied. Finally, the total Δv is recorded, and a report command logs the results. This same sequence is repeated at each TCM, performed at the start of the mission and then at successive planetary periapsis to guide the spacecraft through its flyby chain.

For the Voyager 2 mission, which was replicated first, a test was also conducted to determine whether replacing the targeted loops with optimized loops, removing time constraints, and relaxing constraint tolerances on the B-plane targets would further reduce the required Δv. Since this approach did not yield any improvement in the results, the standard targeted loop structure was retained when modeling Pioneer 11.

All the GMAT scripts and supporting code used in this study are available in the accompanying GitHub repository.[30]

Results and Discussion

Results:

Tables 3 and 4 present the velocity components and corresponding Δv values of the trajectory correction maneuvers (TCMs) for the replicated Voyager 2 and Pioneer 11 missions:

Table 3: Components and Δv of Replicated Voyager 2 Trajectory Correction Manoeuvres.

Burn	Components [m/s]	Δv [m/s]
TCM 1	V: 9.42 N: 5.81 B: -0.79	11.10
TCM 2	V: 32.63 N: 7.35 B: -66.86	74.76
TCM 3	V: 29.71 N: 160.95 B: -163.77	231.53
TCM 4	V: -105.22 N: -345.58 B: 58.82	366.00

Table 4: Components and Δv of Replicated Pioneer 11 Trajectory Correction Manoeuvres.

Burn	Components [m/s]	Δv [m/s]
TCM 1	V: 43.21 N: -12.83 B: -17.38	48.31
TCM 2	V: -959.57 N: 2143.15 B: -266.97	2363.29

When summing the Δv requirements from the replicated manoeuvres, the total values obtained were 683.39 m/s for Voyager 2 and 2411.60 m/s for Pioneer 11. By contrast, the theoretical Δv requirements estimated, as detailed in the Methodology section, from propellant masses and specific impulses were 241.4 m/s for Voyager 2 and 184 m/s for Pioneer 11. Figure 5 below compares these estimated and replicated Δv values for both missions.

DOI: 10.36838/IJHSR87.230

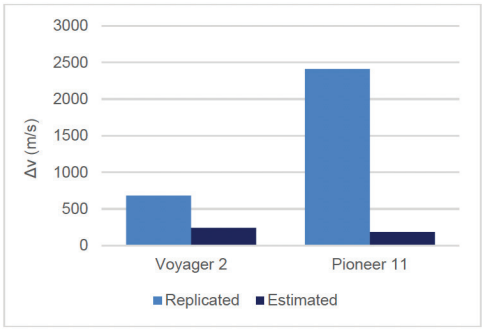

Figure 5: Grouped bar chart comparing the estimated and replicated Δv values for the Voyager 2 and Pioneer 11 missions.

This reveals that the replicated Voyager 2 Δv is 2.83 times larger (283% of the historical estimate, i.e., 183% higher), while the replicated Pioneer 11 Δv is 13.1 times larger (1310% of the historical estimate, i.e., 1210% higher). The significant discrepancies indicate that while the replicated maneuvers reproduce the overall structure of each mission, they overestimate the actual Δv usage by a wide margin.

Discussion:

While this paper is unable to pinpoint with certainty the sources of these discrepancies, there are a number of plausible hypotheses that can be derived from observed patterns in the burn components. Broadly, these discrepancies fall into two categories of error: modeling errors, which stem from the way the mission was represented and solved within GMAT, and computational errors, which arise from the limitations of numerical methods. The following discussion is separated accordingly.

Modeling Errors:

Firstly, for Voyager 2, TCM 4 required a large negative component in the V-direction, while for Pioneer 11, TCM 2 also had a large negative V component. A negative V value means the spacecraft had to reduce its velocity along its trajectory path. In both cases, this suggests that earlier maneuvers had caused the spacecraft to move too fast relative to the planned trajectory. As a result, a large retrograde burn was needed later to correct the speed and ensure the timing of the next planetary encounter remained accurate.

In addition to the V-direction, there were also excessive burns in the B-direction. Both V and B components are used to control the altitude of the flyby at the next planetary encounter. However, due to the Oberth effect, changes in the V-direction (along the velocity vector) are generally more efficient than changes in the B-direction (radial within the orbital plane, perpendicular to V). The fact that GMAT produced comparatively large B burns suggests that the optimization process was not always making use of the most efficient burn orientation. Further inspection of the burn components shows that nearly all B-direction corrections (except for Voyager 2's TCM 4) were negative. This indicates that, instead of relying on altitude-lowering B burns, GMAT could have achieved the same corrections more efficiently by applying retrograde V burns earlier in the trajectory. In the example of Voyager 2, as mentioned earlier, TCMs 1 to 3 all included positive V components that accelerated the spacecraft, which in turn led to a very large retrograde V correction at TCM 4. A more balanced use of retrograde V at earlier stages might have reduced this, as well as the excessive negative B burns. In practice, this could not be mitigated within the adopted methodology, since the simulation would not converge unless all three burn components (V, B, and N) were varied. Moreover, GMAT cannot be made to "see" the mission globally. It can only satisfy one constraint at a time. As a result, suboptimal choices in the early burns accumulate and must be compensated for in subsequent burns, even if that compensation is inefficient.

It was suspected that perhaps these burn choices were forced by the applied constraints. To investigate this possibility, all targeted loops were replaced with optimized loops set to minimize Δv, time constraints were removed, and the B-plane constraints were relaxed to give the optimizer more leeway. However, the simulation consistently converged on the same flyby epochs and produced the same distribution of burn components. This confirms that GMAT's solution, although suboptimal, was the best it could achieve.

In addition to solver inefficiencies, the setup introduced a second type of modeling error: potential mismatches in the BdotT and BdotR constraints. The GMAT replications began with SPICE-derived B-plane targets and epochs, and even tiny mismatches between these and the actual historical encounter values could propagate into significant differences. For instance, the SPK propagator was configured with a one-hour step size. This means that the reported closest-approach BdotT and BdotR values may have fallen in between the sampled points, introducing a small offset from the true values. While this mismatch would likely be minor, such deviations can grow over interplanetary timescales, ultimately magnifying into higher Δv requirements at later encounters. However, due to computational limitations, this study was unable to reduce the step size further to capture the exact closest approach.

Computational Errors:

Another noticeable pattern was the large N-direction burns in both replicated missions. Since the N direction corresponds to out-of-plane maneuvers (perpendicular to the orbital plane), it would be expected that the spacecraft's launch and trajectory geometry would be chosen to already minimize the need for such corrections. These N-direction burns are not only substantial, but also increase in magnitude across both missions. This pattern is also reflected in the trend of increasing Δv at later burns. The first maneuvers in both missions were relatively small, but the later burns grew much larger in magnitude. This behavior is consistent with the surrounding literature on numerical propagation. For instance, a paper on the topic by Mosbach & Turner shows that when differential equations are solved step by step on digital computers, tiny rounding errors accumulate at each integration step. Over the years-long timelines of missions such as Voyager 2 and Pioneer 11, these errors compound, which helps explain why the GMAT replications required progressively larger corrective burns, since the

software's small numerical inaccuracies early in the trajectory snowballed into larger deviations later on.[31]

A potential mitigation strategy for the integration drift problem would be to segment the propagation into shorter spans, rather than attempting to simulate the full mission in a single continuous run. For example, instead of starting from the Earth departure state and propagating all the way to Neptune (Voyager 2) or Saturn (Pioneer 11), one could initialize GMAT at Earth, propagate to Jupiter, and then terminate the sequence. At that point, a new file could be generated, beginning with the spacecraft's SPK-derived state at Jupiter periapsis. This would effectively "reset" the accumulated numerical error at each planetary encounter. By repeating this process, each leg of the mission would be propagated over a much shorter time span, thereby reducing the opportunity for integration drift to compound. In theory, this could yield TCM Δv values much closer to historical estimates. However, such an approach undermines the central aim of this research. The purpose of the study is not simply to reproduce historical trajectories, but to test GMAT's capability as a mission design tool under conditions analogous to planning a future mission. In a real design scenario, trajectory analysts would not have the luxury of resetting the spacecraft's state to "true" values at each encounter, because those values are precisely what the software is meant to predict.

Finally, there is the trade-off between computational accuracy and efficiency. Smaller-step integrators reduce drift but at high computational cost, while larger-step integrators are more efficient but allow small deviations to accumulate. GMAT gives users flexibility in propagator choice and step size, however the extent to which the step size can be reduced will depend on the computational ability of the machine utilized. For this study, the Runge–Kutta propagator was configured with a minimum step size of 60 seconds and a maximum step size of 86400 seconds (1 day). While these values struck a balance between runtime and accuracy on the available computing setup, reducing them could have mitigated integration drift. This opens the door for further investigative work, which could explore systematically varying step size bounds to assess the sensitivity of Δv growth to propagator settings.

■ Conclusion

This study set out to examine the application of NASA's General Mission Analysis Tool (GMAT) in replicating and optimizing historical interplanetary trajectories, using Voyager 2 and Pioneer 11 as case studies. By estimating the historical total Δv required for each mission's TCMs from published fuel mass and engine data, and comparing these against GMAT-simulated equivalents, it was possible to directly assess GMAT's ability to reproduce and/or improve upon past mission performance.

The results showed that GMAT consistently produced significantly higher total TCM Δv than the historical estimates. For Voyager 2, the simulated Δv was nearly three times larger than the estimated real mission value, while for Pioneer 11 it was more than twelve times higher. Analysis of the maneuver components revealed that these discrepancies arose from two primary sources: modeling errors, which stemmed from the way the mission was represented and solved within GMAT through solver choices and constraint inaccuracies, and computational errors, which arose from the way numerical integration accumulates small inaccuracies over long propagation spans, leading to integration drift.

As mentioned in the discussion section, several avenues remain open for further investigation. A logical next step would be to attempt replications using alternative optimization software. NASA's MONTE and Astrogator are both widely used in professional mission planning and may provide more optimal outcomes than GMAT when applied to replicate historical interplanetary trajectories. Furthermore, building on the findings of this paper could be further achieved through a targeted sensitivity analysis to separate the relative impacts of modeling and computational errors. One approach would be to hold all modeling assumptions constant while varying propagator step sizes and length of propagation, thereby isolating the effects of integration drift. Conversely, fixing the propagator configuration while systematically adjusting target constraints and tolerances would reveal how much of the discrepancy stems from the modeling setup. Such an analysis would be particularly valuable in explaining why the replicated Voyager 2 and Pioneer 11 missions diverged so largely in their Δv error margins, despite following similar methodologies. At present, both error sources interact in ways that are difficult to disentangle. Therefore, controlled experiments where one factor is varied, and the other held fixed, would help clarify their relative contributions and provide more concrete guidance on where future tools or methods could improve.

Ultimately, this study has demonstrated that while GMAT is a powerful and accessible tool for modern mission analysis, its use in replicating historical missions exposes limitations in numerical optimization methods when applied to highly constrained, long-duration trajectories. Recognizing these limitations is essential for setting realistic expectations on what such software can achieve, both in revisiting the past and in planning for future interplanetary exploration.

■ Acknowledgments

This research was made possible with the guidance and support of Dr. Steve Bullock and Jacob Higgins at the University of Bristol. I am deeply grateful for their expertise, encouragement, and invaluable feedback throughout the project. I would also like to express my sincere appreciation to my parents for their unwavering support and encouragement, without which this work would not have been possible.

■ References

1. Yefremov, A. P.; Vorobyeva, A. A. A Planet's Gravity Assist as a Powerful Amplifier of Small Physical Effects in the Solar System. *Acta Astronaut.* **2021**, *180*, 205–210. https://doi.org/10.1016/j.actaastro.2020.12.029.
2. *Basics of Spaceflight: A Gravity Assist Primer - NASA Science*. https://science.nasa.gov/learn/basics-of-space-flight/primer/ (accessed 2025-08-14).

DOI: 10.36838/IJHSR87.230

3. NASA. *Pioneer 11 - NASA Science*. https://science.nasa.gov/mission/pioneer-11/ (accessed 2025-08-14).
4. NASA. *Voyager 2 - NASA Science*. https://science.nasa.gov/mission/voyager/voyager-2/ (accessed 2024-12-20).
5. *10 Facts about the Pioneer Spacecraft - NASA Science*. https://science.nasa.gov/missions/pioneer/pioneer-11/10-things-about-pioneer-spacecraft/ (accessed 2025-08-25).
6. Nathan J. Strange. Analytical Methods for Gravity-Assist Tour Design. Dissertation, Purdue University, 2016. https://docs.lib.purdue.edu/open_access_dissertations/852/.
7. General Mission Analysis Tool (GMAT) Product Description. https://ntrs.nasa.gov/api/citations/20080045879/downloads/20080045879.pdf (accessed 2024-12-19).
8. Scott Evans; William Taber; Theodore Drain; Jonathon Smith; Hsi-Cheng Wu; Michelle Guevara; Richard Sunseri; James Evans. Monte: The Next Generation Of Mission Design & Navigation Software. *Jet Propuls. Lab. Inst. Technol.* **2016**.
9. Carrico, J.; Fletcher, E. Software Architecture And Use Of Satellite Tool Kit's Astrogator Module For Libration Point Orbit Missions. In *Libration Point Orbits and Applications*; WORLD SCIENTIFIC: Aiguablava, Spain, 2003; pp 471–487. https://doi.org/10.1142/9789812704849_0021.
10. Shirazi, A.; Ceberio, J.; Lozano, J. A. Spacecraft Trajectory Optimization: A Review of Models, Objectives, Approaches and Solutions. *Prog. Aerosp. Sci.* **2018**, *102*, 76–98. https://doi.org/10.1016/j.paerosci.2018.07.007.
11. Battin. Numerical Integration of Differential Equations. In *An Introduction to the Mathematics and Methods of Astrodynamics, Revised Edition*; AIAA Education Series; American Institute of Aeronautics and Astronautics, Inc., 1999; pp 567–622. https://doi.org/10.2514/5.9781600861543.0567.0622.
12. *General Mission Analysis Tool (GMAT)*. Goddard Engineering and Technology Directorate. https://etd.gsfc.nasa.gov/capabilities/capabilities-listing/general-mission-analysis-tool-gmat/ (accessed 2025-08-22).
13. Hughes, S. P. General Mission Analysis Tool (GMAT), 2016. https://ntrs.nasa.gov/citations/20160003520 (accessed 2024-12-19).
14. Ferrato, E.; Giannetti, V.; Andreussi, T. Guidance, Navigation, and Control of a Low-Altitude Nanosatellite Equipped with Air-Breathing Electric Propulsion. *IEEE Trans. Aerosp. Electron. Syst.* **2025**, 1–16. https://doi.org/10.1109/TAES.2025.3577159.
15. Jared Graef. B-Plane Targeting With The Spacecraft Trajectory Optimization Suite. Thesis, California Polytechnic State University, 2020. https://digitalcommons.calpoly.edu/theses/2251/ (accessed 2025-08-16).
16. Sergeyevsky, A. B.; Snyder, G. C.; Cunniff, R. A. Interplanetary Mission Design Handbook, Volume I, Part 2.
17. Lynam, A.; Didion, A. Impulsive Trajectories from Earth to Callisto-Io-Ganymede Triple Flyby Capture at Jupiter. In *AIAA/AAS Astrodynamics Specialist Conference*; AIAA SPACE Forum; American Institute of Aeronautics and Astronautics, 2014. https://doi.org/10.2514/6.2014-4106.
18. Berg, P. The Fundamental Concepts of the Gravity-Assist Manoeuvre. *Eur. J. Phys.* **2023**, *44* (2), 025002. https://doi.org/10.1088/1361-6404/acaad8.
19. Van Allen, J. A. Gravitational Assist in Celestial Mechanics—a Tutorial. *Am. J. Phys.* **2003**, *71* (5), 448–451. https://doi.org/10.1119/1.1539102.
20. Anderson, J. D.; Campbell, J. K.; Nieto, M. M. The Energy Transfer Process in Planetary Flybys. *New Astron.* **2007**, *12* (5), 383–397. https://doi.org/10.1016/j.newast.2006.11.004.
21. Adams, R.; Richardson, G. Using the Two-Burn Escape Maneuver for Fast Transfers in the Solar System and Beyond. In *46th AIAA/ASME/SAE/ASEE Joint Propulsion Conference & Exhibit*; American Institute of Aeronautics and Astronautics: Nashville, TN, 2010. https://doi.org/10.2514/6.2010-6595.
22. Tsiolkovsky, K. S. Exploration of Outer Space by Means of Rocket Devices.; The Science Review, 1903; Vol. 5.
23. Voyager Backgrounder, 1980. https://ntrs.nasa.gov/citations/19810001583 (accessed 2025-08-18).
24. *Frequently Asked Questions - NASA Science*. https://science.nasa.gov/mission/voyager/frequently-asked-questions/ (accessed 2025-08-18).
25. *Voyager 1 Fires Up Thrusters After 37 Years*. NASA Jet Propulsion Laboratory (JPL). https://www.jpl.nasa.gov/news/voyager-1-fires-up-thrusters-after-37-years/ (accessed 2025-08-18).
26. *4.0 In-Space Propulsion - NASA*. https://www.nasa.gov/smallsat-institute/sst-soa/in-space_propulsion/ (accessed 2025-08-18).
27. Anderson, J. D.; Laing, P. A.; Lau, E. L.; Liu, A. S.; Nieto, M. M.; Turyshev, S. G. Study of the Anomalous Acceleration of Pioneer 10 and 11. *Phys. Rev. D* **2002**, *65* (8), 082004. https://doi.org/10.1103/PhysRevD.65.082004.
28. Turyshev, S. G.; Toth, V. T. The Pioneer Anomaly. *Living Rev. Relativ.* **2010**. https://doi.org/10.12942/lrr-2010-4.
29. *NAIF SPICE Toolkit Hypertext Documentation*. https://naif.jpl.nasa.gov/pub/naif/toolkit_docs/FORTRAN/index.html (accessed 2025-08-22).
30. AdeshKrishnan. AdeshKrishnan/Voyager-2-Pioneer-11-GMAT: V1.0.0, 2025. https://doi.org/10.5281/ZENODO.16927714.
31. Mosbach, S.; Turner, A. G. A Quantitative Probabilistic Investigation into the Accumulation of Rounding Errors in Numerical ODE Solution. *Comput. Math. Appl.* **2009**, *57* (7), 1157–1167. https://doi.org/10.1016/j.camwa.2009.01.020.

Author

Adesh Krishnan is a graduate of St. Joseph's Institution International in Singapore and an aspiring engineer with a strong interest in physics and mathematics. In his free time, he actively expands his technical skill set through online courses in areas such as CAD modeling and programming. He plans to pursue aerospace engineering at university, to apply his interests and skills to make a meaningful contribution to advances in aerospace technology.

Data Availability Statement:

The data supporting the results are available in a public repository at: https://doi.org/10.5281/ZENODO.16927714.